DFT Study of NO Reduction Process on Ag/γ-Al2O3 Catalyst: Some Aspects of Mechanism and Catalyst Structure

DFT Study of NO Reduction Process on Ag/γ-Al_2O_3 Catalyst: Some Aspects of Mechanism and Catalyst Structure

Vitaly E. Matulis[*1], *Ekaterina G. Ragoyja*[1], *Oleg A. Ivashkevich*[2], *Dmitry A. Lyakhov*[3], *Dominik Michels*[3]

[1]Belarusian State University, 4, Nezavisimosti avenue, 220030, Minsk, Republic of Belarus

[2]Research Institute for Physical Chemical Problems of the Belarusian State University, 14, Leningradskaya str., 220006 Minsk, Republic of Belarus

[3]Computer, Electrical and Mathematical Science and Engineering Division, 4700 King Abdullah University of Science and Technology, Thuwal 23955-6900, Saudi Arabia

*e-mail: vitaly_matulis@lyceum.by, +375297504724

Abstract

Catalysts based on $Ag/\gamma\text{-}Al_2O_3$ are perspective systems for practical implementation of catalytic NO reduction. Nevertheless, mechanism and regularities of this process are still not fully investigated. Herein, we present the results of quantum-chemical research of $Ag/\gamma\text{-}Al_2O_3$ catalyst surface and some aspects of NO reduction mechanism on it. Proposed calculation methods using DFT and cluster models of the catalyst surface are compared and verified. The possibility of existence of small adsorbed neutral and cationic silver clusters on the surface of the catalyst is shown. It is demonstrated that NO adsorption on these clusters is energetically favorable, both in the form of monomer and dimer. Scheme of NO selective catalytic reduction (SCR) that explains increasing of N_2O side-product amount on catalysts with silver fraction more than 2 wt% is proposed. The feasibility of this scheme is justified with calculated data. Some recommendations that allow decreasing amount of N_2O are developed.

Keywords: DFT, SCR process, $Ag/\gamma\text{-}Al_2O_3$ catalyst, adsorption, NO reduction mechanism, silver clusters.

1. Introduction

The problem of deteriorating of air quality caused by increasing emission of road transport exhaust gases is especially urgent nowadays. Therefore, many researchers are focused on development of new effective catalysts for afterburning of fuel residues and reduction of nitrogen oxides. In particular, it has been shown that silver particles adsorbed on the surface of aluminium oxide catalyze the selective reduction of nitrogen oxides.[1] Obviously, the catalytic activity of such systems depends on the size and the charge of the adsorbed silver particles. Therefore, it is important to know how these characteristics affect the SCR process. Based on the results of experimental and theoretical investigations Deng et al[2] have shown that for high efficiency of the SCR process, the optimal concentration of silver in the catalyst should be within 1-2 wt%. Data from photoelectron spectroscopy, EXAFS and XANES testifies that below 2 wt% single silver atoms and Ag^+ cations act as catalytic centers in SCR. At the same time, when silver mass fraction exceeds 2 wt%, Ag–Ag bonds are formed, which leads to the formation of silver clusters on the surface. Thus, using DFT calculations Deng et al have shown that structures with Ag^+, $Ag_2^{\delta+}$, $Ag_3^{\delta+}$ and $Ag_4^{\delta+}$ silver particles adsorbed on the γ-Al_2O_3 surface match the experimental data. Therefore, silver atoms and cations, as well as small neutral and positively charged silver clusters, adsorbed on the γ-Al_2O_3 surface should be considered as catalytic centers in SCR. For the best of our knowledge, there is no information about adsorption energies of small neutral silver clusters on γ-Al_2O_3 surface in the literature.

Nitrogen monoxide adsorption on the catalyst surface plays a key role in SCR mechanism. Experimentally this process has been studied by Müslehiddinoğlu et al[3] on Ag/α-Al_2O_3. Their results demonstrate that NO undergoes dissociation on the catalyst surface at 300 K. Consequently, silver particles are oxidized, and N_2O is formed. Liu et al[4] have carried out a

theoretical study of NO adsorption on Ga/Al_2O_3. They have shown that along with adsorption on gallium-containing centers, NO adsorption on bare Al_2O_3 surface is also likely.

Mechanism of SCR process on $Ag/\gamma\text{-}Al_2O_3$ catalyst is still unclear. Nevertheless, some important intermediates on the catalyst surface have been detected by IR-spectroscopy. There are isocyanates[5], organic nitro compounds[6], nitriles[7], ammonia[8], acetates[9], nitrates[9] and enolates[10] among them. Several reaction schemes involving mentioned intermediates have been proposed.[11,12] Lee and coworkers[13] have suggested a bifunctional version of SCR stages localization. According to them, NO and hydrocarbons turn into NO_2 and reactive hydrocarbon derivatives on silver-containing sites, whereas subsequent reactions between these intermediates occur on different sites of catalyst surface, including bare Al_2O_3. Predominance of one intermediate or another is determined by the composition of the initial reaction mixture[12] and the structure of the catalyst. Regularities that explain how the composition of the initial system influences the composition of the formed intermediates and products have not yet been established. However, it has been shown[9] that amount of side-product N_2O increases when silver mass fraction in the catalyst is greater than 2 wt%. One of the goals of our work was to elucidate this intriguing fact.

To summarize, there are scattered experimental data on SCR processes in the literature. Therefore, the mechanism of SCR, as well as the main factors affecting the process efficiency, has not yet been clarified. The data of theoretical investigations of SCR processes and the structure of corresponding catalysts are also meager. At the same time, information about the energy characteristics, geometry and electronic structure of the catalytic systems, derived from quantum-chemical calculations, is crucial for understanding of the mechanism of the SCR process. Accordingly, the aim of this work is to study the surface of $Ag/\gamma\text{-}Al_2O_3$ catalyst as well

as some aspects of the mechanism of the SCR process on this catalyst by means of quantum chemistry.

2. Computational details

All the calculations were carried out using DFT approach. Firstly, the geometry and energy characteristics of silver clusters were calculated using 12 DFT functionals. Calculations of characteristics of isolated silver clusters instead of aluminium oxide surface were chosen for the preliminary selection of the functionals because it is more problematic to obtain accurate and reliable results for systems with heavy elements. Based on the obtained data (see section 3.1 and Supporting Information), TPSSh[14] functional and SDD[15] basis set for silver atoms were chosen for further calculations.

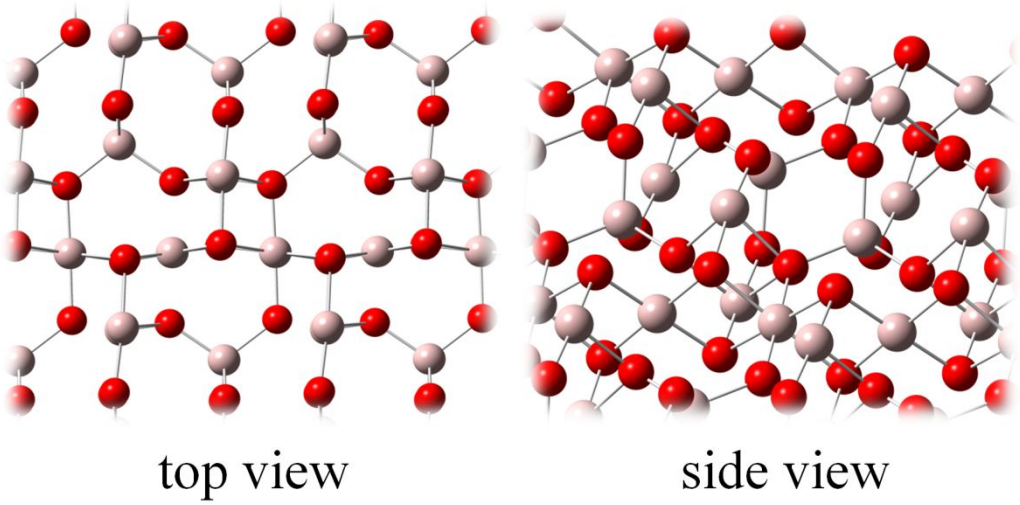

Figure 1. Structure of the (110) γ-Al_2O_3 surface. Color legends: red for oxygen atoms and light pink for aluminium atoms.

Simulation of crystal surfaces and surface processes is one of the most challenging problems in quantum chemistry. There are two main approaches to such simulations: periodic and cluster models of the surface,[16] the latter was used in this work. Crystallographic data on γ-Al_2O_3 structure was taken from work.[17] In γ-Al_2O_3 (110) surfaces account for 70-83% of the total surface area, while the remaining part is occupied mostly by (100) surfaces.[18] Thus, we chose the (110) surface for simulation of the γ-Al_2O_3 surface. This surface is shown in Figure 1. Based on the (110) surface, 5 cluster models were created. Structures and formulas of all the models are presented in Figure 2. Model 1 is a saturated cluster model, which does not fully reflect the structure of the surface. Due to its small size this model was used for comparative calculations within DFT and coupled cluster theory approaches (see Supporting Information). Based on these calculations, 6-311G* basis set[19,20] was chosen for Al, O, and H atoms for further investigation. The accuracy of results obtained with chosen TPSSh/6-311G* level of theory have also been justified by comparison with data obtained with higher level of theory – CCSD(T).[21] More details are provided in Supporting Information.

Models 2 and 3 have similar structure. Both of them are parts of the (110) surface, but model 2 is a regular bare cluster model, while model 3 has all dangling bonds saturated with hydrogen atoms. Both models are neutral. Coordinates of atoms at the edges of these models were frozen during geometry optimization in order to prevent folding of the surface.

It is worth noting, that the first three models don't take in account the influence of the bulk crystal on adsorption center on the surface. To consider this influence, two more cluster models were proposed. Both models 4 and 5 are embedded into the array of point charges with values of +3 and -2, which are situated at corresponding positions of Al^{3+} and O^{2-} ions in bulk crystal. Model 4 includes 10 aluminium atoms, while model 5 includes 22 aluminium atoms. All oxygen

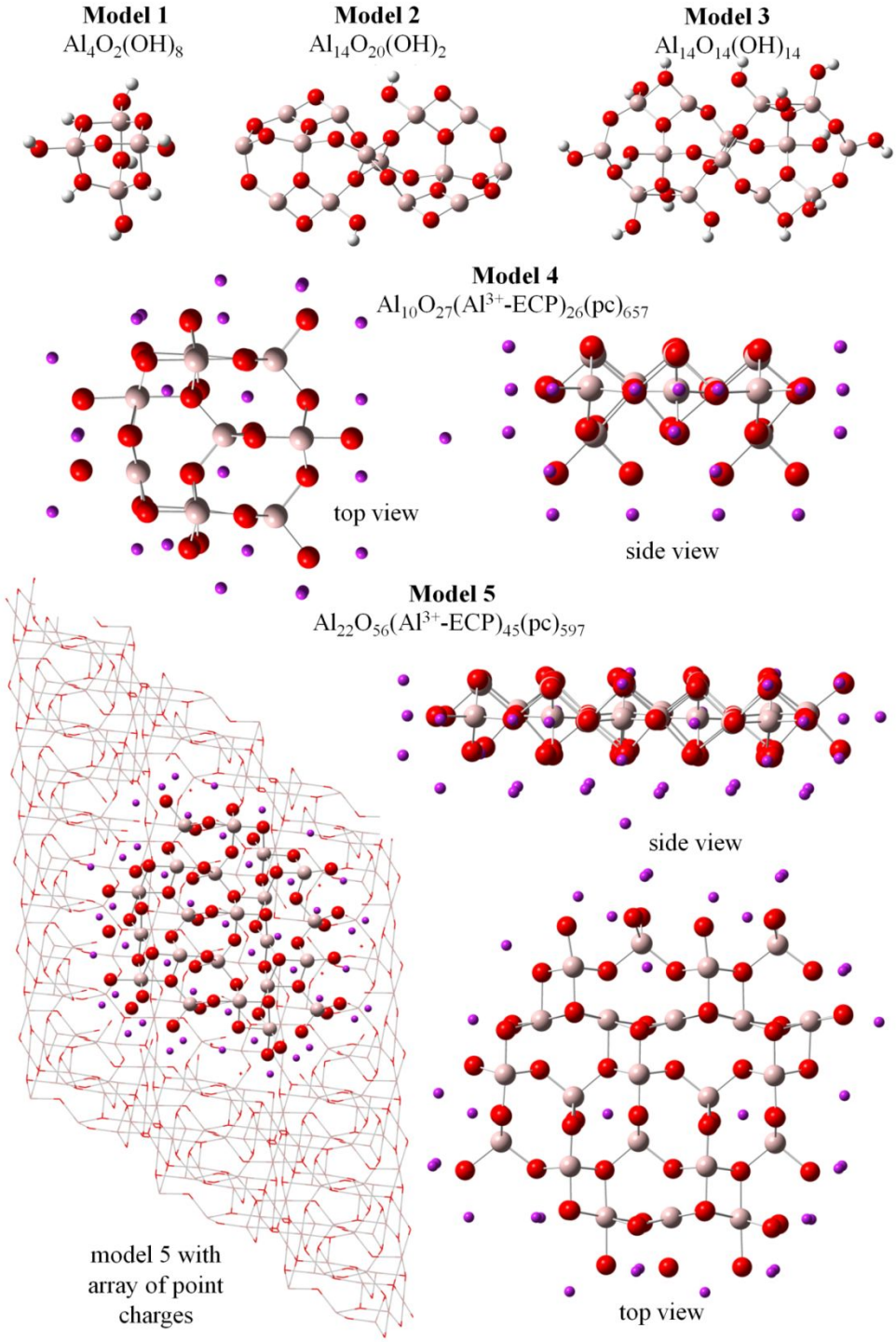

Figure 2. The proposed cluster models of the γ-Al_2O_3 surface. Color legends: red for oxygen atoms, light pink for aluminium atoms, white for hydrogen atoms, and purple for "soft" charges. In top and side views of models 4 and 5 point charges were omitted for clarity.

atoms that are connected with these aluminium atoms are also included into the cluster model. "Soft" charges were used in order to avoid distortion of the structures on the edges and subsequent need for freezing of atoms coordinates during optimization. "Soft" charges are Al^{3+} ions that are described only by ECP[22] without any basis functions. They were placed on Al^{3+} positions in bulk crystal structure between cluster model atoms and point charges (Figure 2). This approach prevents excessive polarization of cluster model atoms by point charges. Similar technique was used in some other works.[23,24] The whole embedded cluster models 4 and 5 (together with corresponding array of point charges) are neutral. During geometry optimization coordinates of point charges and "soft" charges were frozen.

All the proposed models of γ-Al_2O_3 surface are analyzed and compared in section 3.2.

Energies of adsorption of different molecules on the surface of the catalyst were calculated as follows:

$$E_{ads} = E_{adsorbate\ on\ surface} - E_{isolated\ adsorbate} - E_{surface}$$

The negative adsorption energy value indicates that the adsorbed state is energetically favorable. Zero point vibrational energy wasn't taken into account. Calculations of all adsorption or dissociation energies were performed with the basis set superposition error (BSSE) correction. The BSSE correction was calculated according to counterpoise correction procedure[25] as follows:

$$\Delta W_c = \left(W_1^* - W_1\right) + \left(W_2^* - W_2\right),$$

where ΔW_c is the BSSE correction energy itself; W_1 and W_2 are energies of both reactants (isolated adsorbate and isolated surface), which have geometries as in the complex (adsorbate on surface), calculated with their corresponding original basis sets; W_1^* and W_2^* are energies of the same structures calculated with modified basis sets that include basis functions of both reactants

(adsorbate and surface). That is, for isolated adsorbate, W_1^* is calculated using original basis set of the adsorbate with added basis functions of the atoms of the surface. These added basis functions are localized at points where atoms of the surface are situated in the complex (adsorbate on surface).

All the calculations were carried out using Gaussian16 program.[26]

3. Results and discussion

3.1 Isolated silver clusters

The calculations of geometry and several energy characteristics of small silver clusters were carried out to reveal the best calculation method for the further study (see Supporting Information for details). Firstly, bond length in Ag_2 was calculated using 12 different DFT functionals and cc-pVTZ-PP basis set[27]. The calculated values were compared with the experimental one[28] and with the value obtained with CCSD(T,Full) method. Almost in all cases bond length was overestimated by DFT. Nevertheless, four functionals, that gave the best results, were chosen for further calculations: TPSSh, B3PW91[29], M06[30] and PBE0.[31] Then accuracy of the chosen functionals was estimated by calculations of some energy characteristics of Ag_2: vibrational frequency, dissociation energy and ionization potential, as well as vertical detachment energy of Ag_2^-. Four basis sets: cc-pVTZ-PP, SDD, LanL2DZ[32] and LanL2TZ[32,33] were used for the mentioned calculations. The results of calculations were compared with the experimental ones.[28,34] It has been found that TPSSh and M06 functionals are more accurate than PBE0 and B3PW91. The combination of TPSSh functional and SDD basis set performed best in vibrational frequency and dissociation energy prediction. Finally, to choose between M06 and TPSSh, transition energies of photoelectron spectra of Ag_2^- — Ag_5^- anions and dissociation

energies of some neutral and anionic silver clusters were calculated and compared with experimental data.[34] Despite in work[35] M06 functional is stated to be the most accurate for silver clusters, our data shows that TPSSh is more precise. Apart from that, Ag_3 geometry predicted in M06 is different from the structure widely accepted in the literature.[36] Thus, obtained data allows us to choose TPSSh as more preferable for the goals of our study.

SDD basis set was chosen for silver atoms, because it enables to get accuracy close to larger basis sets with less demand on CPU time. The TPSSh/SDD optimized geometries of isolated silver clusters and the corresponding total energies were used in subsequent parts of this work.

All the data discussed in this section can be found in Supporting Information.

3.2 Comparison of the (110) γ-Al_2O_3 surface models

For comparison of the proposed models of the (110) γ-Al_2O_3 surface HOMO-LUMO gaps, as well as Ag_2 and Ag_2^+ adsorption energies were calculated (Table 1 and Figure 3). To compute the adsorption energy of Ag_2^+ the total charge of the isolated silver dimer as well as the total charge of the system consisting of silver dimer adsorbed on Al_2O_3 was set as +1. In the case of cluster models, HOMO-LUMO gap approximates the band gap of the γ-Al_2O_3 crystal. Models with too small HOMO-LUMO gap value are likely to provide unreliable description of surface properties. Experimental band gap value is 7.6±0.1[37] eV. Values obtained in periodic calculations are functional-dependent: 3.9−4.9 eV (PW91 with plane waves basis set), 5.86 eV (PBEPBE/6-31G) and 7.64 eV (MN12-L/6-31G).[17] As it can be seen from Table 1, all models, except model 2, have HOMO-LUMO gap values comparable with periodic calculations results.

Table 1. The values of HOMO-LUMO gaps and adsorption energies of Ag_2 and Ag_2^+ calculated for proposed cluster models of the (110) γ-Al_2O_3 surface (see Figure 2).

Model	HOMO-LUMO gap, eV	Ag_2 adsorption energy, kJ/mol [a]	Ag_2^+ adsorption energy, kJ/mol [a]
1 $Al_4O_2(OH)_8$	5.31	-61.10 (20.33)	-150.80 (23.60)
2 $Al_{14}O_{20}(OH)_2$	2.48	-57.35 (19.96)	-275.31 (23.17)
3 $Al_{14}O_{14}(OH)_{14}$	3.95	-64.40 (25.62)	-229.33 (26.31)
4 $Al_{10}O_{27}(Al^{3+}\text{-ECP})_{26}(pc)_{657}$	4.71	-119.50 (60.56)	-357.56 (55.40)
5 $Al_{22}O_{56}(Al^{3+}\text{-ECP})_{45}(pc)_{597}$	4.33	-128.51 (51.63)	-359.05 (54.72)

[a] The adsorption energies are given with BSSE taking into account. The BSSE values are provided in brackets.

There is no experimental data for neutral and cationic silver dimers adsorption energies, but there are some results of periodic calculations for similar systems. Thus, the calculated $Ag_2^{\delta+}$ adsorption energy on the (110) γ-Al_2O_3 surface is mentioned to be -292 kJ/mol[2], while Ag_2 adsorption energy on α-Al_2O_3 is estimated to be -114 kJ/mol.[38] Our results show that embedded cluster models 4 and 5 predict adsorption energy values that are comparable with data of periodic calculations (Table 1). Moreover, values obtained for models 4 and 5 are close to each other, unlike the values obtained with other models. The adsorption energies of Ag_2^+ cluster are far more negative than of Ag_2. Such huge difference in the adsorption energies is explained by increased stability of neutral silver dimer, which has two electrons in the outer shell. It is well known, that silver clusters with 2, 8, 18 etc. 5*s*-electrons in the outer shell possess the increased stability (similarly to atoms of noble gases).[36]

It should be noted, that the adsorption energy values calculated for different models vary greatly. It can be explained by different location of the adsorbate in relation to the surface. Model 1 is too small for both silver atoms to interact with the surface simultaneously (see Figure 3).

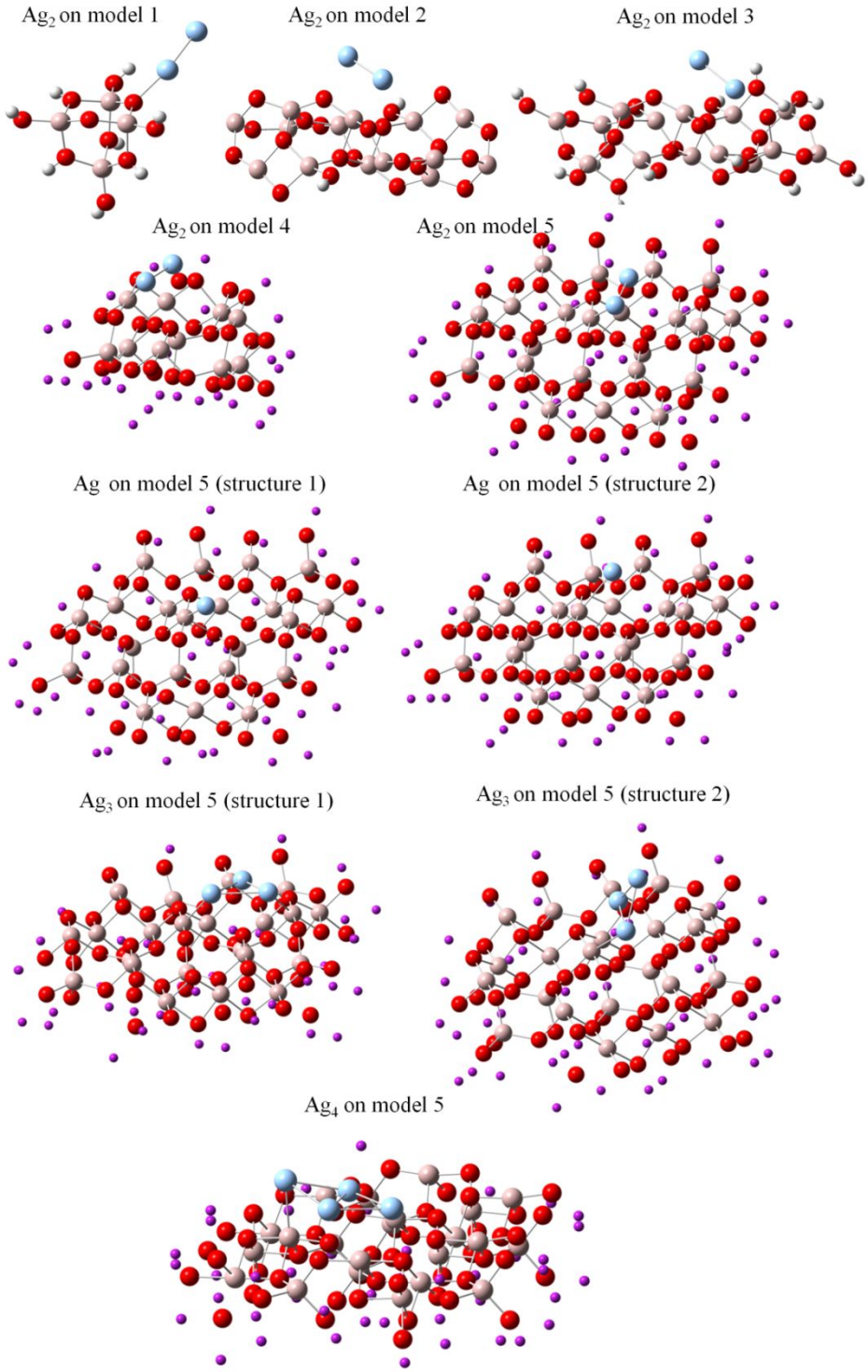

Figure 3. The calculated structures of silver particles adsorbed on different cluster models of the (110) γ-Al_2O_3 surface. Color legends: red for oxygen atoms, light pink for aluminium atoms, purple for "soft" charges, white for hydrogen atoms, and light blue for silver atoms.

Models 2–5 are large enough for silver dimers to adsorb by both atoms at the same time. Nevertheless, models 2 and 3 are revealed to be unable to fully reproduce the adsorption site. Each silver atom of the dimer adsorbed on these models has only one oxygen atom in coordination, while in case of models 4 and 5 each silver atom in dimer is coordinated with two oxygen atoms (Figure 3).

We have concluded that embedded cluster models 4 and 5 are the best for (110) γ-Al_2O_3 surface properties prediction among the models proposed in this paper. The larger model 5 is the most suitable for the study of SCR mechanism, because it reproduces the adsorption site most comprehensively. It is worth pointing out, that the proposed embedded cluster models of the (110) γ-Al_2O_3 surface allow obtaining accurate results with much less computational cost in comparison with hybrid DFT periodic models.

3.3 Silver particles adsorbed on the (110) γ-Al_2O_3 surface

Adsorption of neutral Ag_1 – Ag_4 particles and cations Ag^+ and Ag_2^+ on the (110) γ-Al_2O_3 surface was studied using cluster model 5. The obtained results are given in Table 2. The optimized structures of neutral silver particles absorbed on the (110) γ-Al_2O_3 surface are presented in Figure 3. It should be noted, that the calculations using model 4 predicted nearly the same geometries and adsorption energy values, these results are provided in Supporting Information.

Several minima corresponding to different position of silver particles in relation to the surface were obtained during geometry optimization in the case of Ag and Ag_3 adsorption. For Ag_3 these minima correspond to structures with different number of silver atoms that take part in binding to the γ-Al_2O_3 surface. As expected, adsorption energy and BSSE values are correlated with this

number. The more silver atoms are bound to the surface, the higher (in absolute value) is the adsorption energy and the higher is the BSSE value. This regularity is connected with differences in distance between the cluster and the surface as well as with corresponding overlap of their basis functions.

In all considered cases, the calculated adsorption energy values are large negative numbers (Table 2). It can be seen from Table 2 that the calculated values of adsorption energies of silver particles Ag_n increase (in absolute value) with increasing of number of silver atoms (n). This result is in agreement with our previous calculations of adsorption energy of Ag_2, Ag_4 and Ag_8 on TiO_2 surface.[24,39,40] It should be noted, that according to our calculations the adsorption of Ag_2 and Ag_4 on γ-Al_2O_3 is more favorable than on TiO_2.[24,39,40]

Table 2. The calculated adsorption energy values of neutral and cationic silver particles on the (110) γ-Al_2O_3 surface.

Adsorbate	Model 5	
	Adsorption energy, kJ/mol [a]	Adsorption energy, kJ/mol/atom
Ag (structure 1)	-67.85 (28.27)	-67.85
Ag (structure 2)	-49.27 (28.95)	-49.27
Ag_2	-128.51 (51.63)	-64.26
Ag_3 (structure 1)	-198.52 (73.63)	-66.17
Ag_3 (structure 2)	-166.54 (62.21)	-55.51
Ag_4	-256.96 (97.23)	-64.24
Ag^+	-351.56 (28.85)	-351.56
Ag_2^+	-359.05 (54.72)	-179.53

[a] The adsorption energies are given with BSSE taking into account. The BSSE values are provided in brackets.

In spite of the formation of silver clusters on the surface of γ-Al_2O_3 is energetically favorable, the adsorption energy per number of silver atoms in cluster slightly decreases with growth of the cluster size. This fact may indicate the possibility of dissociation of the adsorbed silver clusters on the γ-Al_2O_3 surface. Such possibility was examined by building corresponding energy diagrams (Figure 4). Values on the diagrams which are highlighted in blue are the results of quantum-chemical calculations. Values which are highlighted in red are the dissociation energies of the corresponding adsorbates on the γ-Al_2O_3 surface. These values were obtained from the diagrams on the basis of the Hess's law. All the considered dissociation processes were found to be endothermic. Thus, according to our calculations there is a high probability of existence of the small silver clusters on the catalyst surface. This allows considering such adsorbates as active catalytic centers in SCR process. It is worth noting that reverse process (clusters aggregation) is unlikely, because real catalyst is prepared by methods that ensure clusters remoteness from each other.

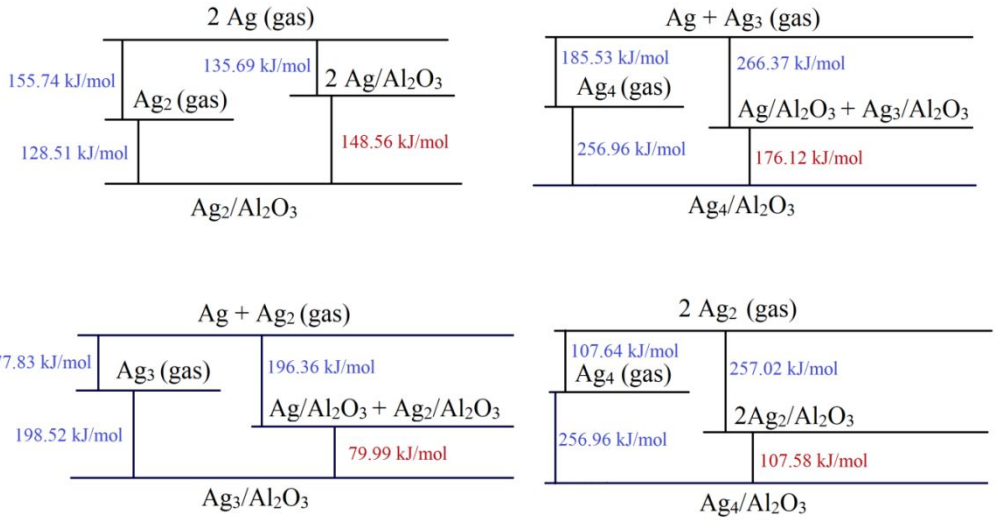

Figure 4. Energy diagrams for calculations of the adsorbed silver clusters dissociation energies.

3.4 NO adsorption on the catalyst surface

The adsorption of NO on different sites of the catalyst was studied. It should be noted that calculations using models 4 and 5 predict nearly the same geometries of the adsorbates. The optimized within model 4 adsorbates structures, as well as the adsorption energies are given in Supporting Information. In case of NO adsorption on Ag_2^+, both triplet and singlet states were considered. Our DFT and CCSD(T) calculations demonstrate that singlet state has lower energy.

The calculated within models 2 and 5 adsorption energies of NO molecule on $Ag_2/\gamma\text{-}Al_2O_3$, $Ag_2^+/\gamma\text{-}Al_2O_3$, as well as on isolated neutral and positively charged silver dimers are given in Table 3. We used model 2 along with model 5, since model 2 is simpler and will probably be used by us to calculate the kinetic parameters of the SCR process in the future. As it can be seen from Table 3, the calculated within model 5 values of adsorption energy are close to our calculated value of NO adsorption energy on the bare (110) $\gamma\text{-}Al_2O_3$ surface (-52.38 kJ/mol, for details see Supporting Information). All the mentioned processes are energetically favorable. Moreover, NO adsorption on isolated silver clusters (Table 3) is less favorable than on clusters adsorbed on $\gamma\text{-}Al_2O_3$. The calculations within model 2 predict NO adsorption both on Ag_2/Al_2O_3 and Ag_2^+/Al_2O_3 to be more favorable in comparison with results obtained with model 5. It should be noted that the calculated within model 5 value of adsorption energy of NO (-54.75 kJ/mol, Table 3) on $Ag_2/\gamma\text{-}Al_2O_3$ is close to our previously calculated value of NO adsorption energy on Ag_2/TiO_2 (110) rutile (53.1 kJ/mol).[41]

We can conclude that on real catalyst surface NO molecules are able to adsorb both on the $\gamma\text{-}Al_2O_3$ surface itself and on the adsorbed silver clusters. Therefore, it is reasonable to consider SCR schemes that include NO adsorption with subsequent conversion of the adsorbates.

3.5 Some aspects of the NO reduction mechanism

In the case of NO reduction mechanism, we aimed to explain how the increased silver concentration causes the growth of the amount of side-product (N_2O). It has been shown, that the nature of the silver-containing centers changes from single silver atoms or cations to clusters when concentration of silver in the catalyst exceeds 2 wt%.[2] Broadening of the silver-containing center extremely widens the range of possible reactions on it. Particularly, NO dimerization that is observed on bulk silver at low temperatures[42] may occur. The produced dimer N_2O_2 can easily transmit oxygen atom to other molecules to form N_2O. An acetaldehyde molecule can act as such acceptor of the oxygen atom. It is assumed that acetaldehyde is formed during the SCR process from ethylene or ethanol in the gas phase.[13] Presence of acetaldehyde in the SCR reaction mixture has been demonstrated experimentally.[43] Based on the above considerations, we have proposed a reaction scheme for explanation of the experimental data (Figure 5).

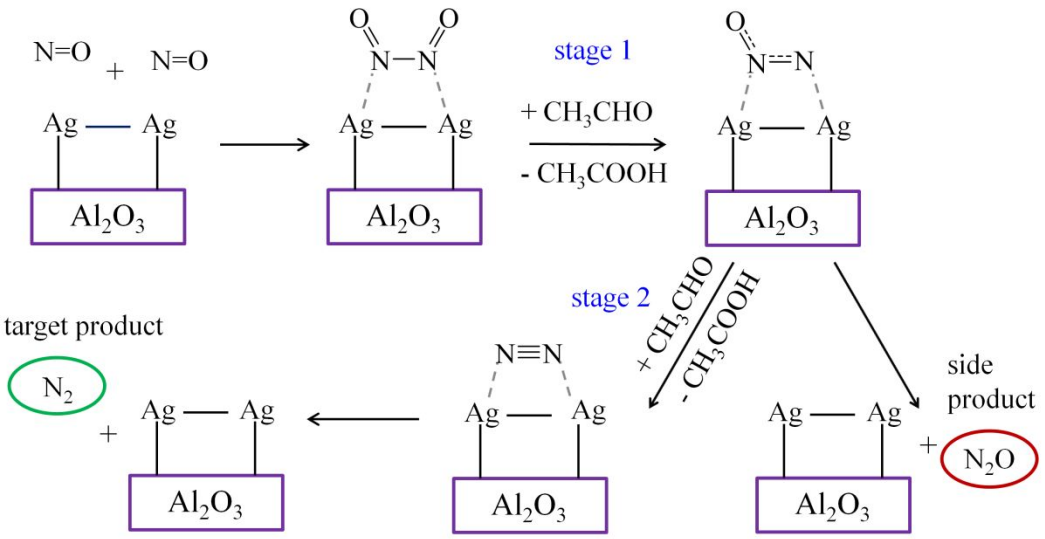

Figure 5. The proposed scheme of NO reduction with acetaldehyde on Ag/γ-Al_2O_3.

Table 3. The calculated values of total energy change for all stages of the proposed reaction scheme (Figure 5).

Process	Isolated silver clusters	Adsorbed silver clusters (model 2)	Adsorbed silver clusters (embedded model 5)
NO adsorption energy, kJ/mol [a]	Ag_2: -29.43 (9.03) Ag_2^+: -58.65 (8.66)	Ag_2: -81.53 (12.83) Ag_2^+: -66.04 (13.02)	Ag_2: -54.75 (12.42) [b] -45.56 (11.91) [b] Ag_2^+: -59.86 (13.25)
(adsorption energy of two NO molecules with dimer formation) - 2·(adsorption energy of single NO molecule), kJ/mol [f]	Ag_2: +20.25 Ag_2^+: -12.49	Ag_2: -6.53 Ag_2^+: -77.82	Ag_2: -13.78 [b] -32.16 [b] Ag_2^+: -69.82
total energy change of stage 1 (see Figure 5), kJ/mol	Ag_2: -97.13 [c] -304.81 [c] Ag_2^+: -270.72	Ag_2: -126.22 Ag_2^+: -132.14	Ag_2: -127.46 Ag_2^+: -161.04 [d] -179.12 [d]
total energy change of stage 2 (see Figure 5), kJ/mol	Ag_2: -488.39 [c] -280.90 [c] Ag_2^+: -271.30	Ag_2: -229.54 Ag_2^+: -244.01	Ag_2: -397.09 [e] -394.66 [e] Ag_2^+: -283.25 [d] -265.16 [d]
N_2O adsorption energy, kJ/mol [a]	Ag_2: +207.50 (14.41) [c] -11.75 (5.68) [c] Ag_2^+: -58.10 (6.49)	Ag_2: +49.51 (15.99) Ag_2^+: +2.49 (15.23)	Ag_2: +94.41 (20.82) Ag_2^+: -8.11 (17.29) [d] -26.35 (17.14) [d]
N_2 adsorption energy, kJ/mol [a]	Ag_2: -5.61 (7.70) Ag_2^+: -40.39 (8.29)	Ag_2: +102.34 (11.16) Ag_2^+: +41.86 (11.41)	Ag_2: -25.60 (10.70) [e] -19.14 (14.73) [e] Ag_2^+: -10.89 (10.56)

[a] The adsorption energies are given with BSSE taking into account. The BSSE values are provided in brackets.

[b] Values corresponding to two different structures of NO adsorbate are given.

[c, d] Values corresponding to two different structures of N_2O adsorbate are given.

[e] Values corresponding to two different structures of N_2 adsorbate are given.

[f] This value of energy difference shows in which form NO adsorption is more favorable. Negative values mean that adsorption of NO in the form of dimer is more favorable.

Both neutral and cationic silver dimers were considered as catalytic centers on the proposed scheme. Total energy change values were calculated for all stages of the reaction scheme to examine the relevance of the proposed element of the SCR mechanism. The calculations were carried out both for isolated silver clusters and for clusters adsorbed on the γ-Al_2O_3 surface. For comparison, both embedded (model 5) and bare (model 2) cluster models were used for calculations. The results of the calculations are given in Table 3. The optimized structures of adsorbates are given in Figs 6 – 8 of Supporting Information.

As it can be seen from the Table 3, NO adsorption with dimer formation is more favorable on the supported silver clusters than on isolated ones. Based on the calculated value for Ag_2^+/γ-Al_2O_3 within model 5, we can conclude that existence of N_2O_2 adsorbates on the catalyst surface is still more favorable (in comparison with adsorbed monomers) at the temperatures up to 400 K. This temperature was estimated based on the calculated entropy of NO dimerization.[44] The calculated energy difference value in the case of neutral silver dimer is less negative. Such small energy profit is unable to compensate for the entropy decreasing with NO dimerization. Thus, the formation of N_2O_2 during adsorption is likely to occur only on positively charged supported silver clusters.

According to our calculations both N_2 and N_2O formation processes (stages 1 and 2) are exothermic (see Table 3). That means that reaction should not finish on the stage of N_2O formation. Moreover, the second stage is more energetically favorable due to formation of very stable nitrogen molecule. Nevertheless, experimental data shows that N_2O is obtained.[9] To understand this regularity, desorption process of the products was studied. The calculated adsorption energy values (Table 3) show that N_2O adsorption on supported silver clusters is less favorable than adsorption of NO both as monomer or with dimer formation. Consequently, N_2O

that is formed during the stage 1 is likely to desorb from the catalyst surface before the conversion into N_2. An additional argument for the proposed explanation is the fact that initially formed N_2O isomer with angular structure (see stage 1 in Figure 5) has less negative adsorption energy (Figure 6).

In the view of kinetics, the proposed interpretation is also reasonable. The conversion of N_2O into N_2 is a long process which requires one more acetaldehyde molecule to get close to the reaction center in a right spatial orientation, whereas desorption of the N_2O molecule is a much faster process. We have also estimated the reaction barriers for the proposed mechanism by performing calculations on the isolated silver clusters. The reaction barriers for N_2O formation were found to be 50-70 kJ/mol, while N_2 formation involves barriers up to 100 kJ/mol (unpublished results). Such barriers are easy to overcome taking into account that the reaction is carried out at a high temperature. The whole mechanism will be thoroughly studied in the future.

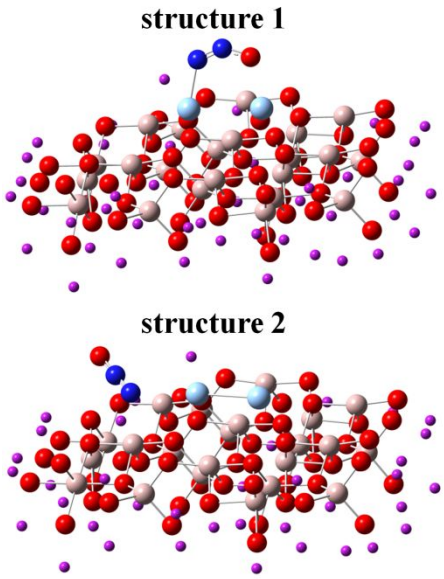

Figure 6. The optimized structures of N_2O adsorbates on $Ag_2^+/\gamma\text{-}Al_2O_3$ (model 5). Color legends: red for oxygen atoms, light pink for aluminium atoms, purple for "soft" charges, blue for nitrogen atoms, and light blue for silver atoms.

Thus, we have demonstrated that the proposed reaction scheme is reasonable and capable to explain the experimental facts. Our data testify that such reactions are more likely to occur on positively charged silver clusters such as Ag_2^+.

It should be noted, that in case of N_2O and N_2 calculated adsorption energies obtained using model 2 are quite different from the results obtained with model 5. Despite optimized geometries of different adsorbates are similar for the both models, model 2 predicts endothermic adsorption of N_2O and N_2 both on neutral and cationic supported silver dimers. Obviously such situation is barely possible in reality. If adsorption without dissociation or significant molecule distortion occurs, dispersion attractive forces make the main contribution to the interaction. These forces make adsorption exothermic even in case of such inert species as N_2[45] and molecules of noble gases.[46] Mentioned differences between two models can be explained by the fact that model 2 contains dangling bonds and doesn't take into account the influence of the bulk crystal on adsorption centers on the surface. For these reasons, model 5 was preferred for the results interpretation.

4. Conclusions

The comprehensive quantum-chemical study of structure and properties of $Ag/\gamma\text{-}Al_2O_3$ catalyst has been carried out. It was shown and justified that TPSSh functional with SDD and 6-311G* basis sets is a good choice for the prediction of the geometry and energy characteristics of the mentioned systems. Five different cluster models were proposed to simulate the (110) $\gamma\text{-}Al_2O_3$ surface. Our data shows that the most reliable results could be obtained within embedded cluster models with "soft" charges (models 4 and 5 on Figure 2). Our results show that proposed

embedded cluster models allow to obtain results that are comparable with data of periodic calculations, but with much less computational cost.

The nature of silver-containing catalytic centers on the surface was also studied. The existence of neutral and positively charged small silver clusters on the γ-Al_2O_3 surface was demonstrated based on the calculated adsorption and dissociation energies. The obtained results are consistent with experimental data. The adsorbed silver clusters Ag_2 – Ag_4 were found to be stable towards dissociation on the γ-Al_2O_3 surface. Our calculations indicate that NO adsorption both on silver-containing centers and on the bare γ-Al_2O_3 surface is favorable.

We have also proposed the reaction scheme of SCR for Ag/γ-Al_2O_3 catalysts with silver fraction more than 2 wt%. The proposed scheme involves NO adsorption on Ag_2^+ centers with N_2O_2 formation and further transmission of the oxygen atoms to produce N_2O or N_2. The feasibility of the scheme was shown based on our calculated data. According to our data in the case of supported silver clusters as catalytic centers, the amount of side-product N_2O increases because of favorable desorption of N_2O from the catalyst surface. The proposed reaction scheme clarifies the experimental data known from the literature.

We hope that our results will be useful and significant for further elucidation of the SCR mechanism. The information on the mechanism would make possible to develop practical recommendations on optimization of the SCR process. Our results allow doing it even at the current stage. Namely, we suggest that low silver fraction in the catalyst along with higher temperature of the process will decrease the amounts of N_2O side product.

Supporting Information

Calculated data for isolated silver clusters obtained with different methods; optimized coordinates of all the surface models proposed; calculated adsorption energies of neutral and

cationic silver clusters on (110) γ-Al_2O_3 surface (model 4); calculated dissociation energies of adsorbed silver clusters on (110) γ-Al_2O_3 surface (model 5); energy and geometric parameters of NO adsorbed on different sites of the catalyst surface (calculated using model 4); optimized structures of various adsorbates.

Acknowledgement

All Gaussian16 computations were performed on KAUST's Ibex HPC. We thank the KAUST Supercomputing Core Lab team for assistance with execution tasks on Skylake nodes.

References

(1) Shimizu, K. I.; Satsuma, A.; Hattori, T. Catalytic Performance of Ag–Al_2O_3 Catalyst for the Selective Catalytic Reduction of NO by Higher Hydrocarbons. *Appl. Catal. B* **2000**, *25*, 239-247.

(2) Deng, H.; Yu, Y.; Liu, F.; Ma, J.; Zhang, Y.; He, H. (2014). Nature of Ag Species on Ag/γ-Al_2O_3: a Combined Experimental and Theoretical Study. *ACS Catal.* **2014**, *4*, 2776-2784.

(3) Müslehiddinoğlu, J.; Vannice, M. A. Adsorption of NO on Promoted Ag/α-Al_2O_3 Catalysts. *J. Catal.* **2003**, *217*, 442-456.

(4) Liu, Z.; Ma, L.; Junaid, A. S. NO and NO_2 Adsorption on Al_2O_3 and Ga Modified Al_2O_3 Surfaces: a Density Functional Theory Study. *J. Phys. Chem. C* **2010**, *114*, 4445-4450.

(5) Ukisu, Y.; Miyadera, T.; Abe, A.; Yoshida, K. Infrared Study of Catalytic Reduction of Lean NO_x with Alcohols over Alumina-supported Silver Catalyst. *Catal. Lett.* **1996**, *39*, 265-267.

(6) Kameoka, S.; Chafik, T.; Ukisu, Y.; Miyadera, T. Role of Organic Nitro compounds in Selective Reduction of NO_x with Ethanol over Different Supported Silver Catalysts. *Catal. Lett.* **1998**, *51*, 11-14.

(7) Gorce, O.; Baudin, F.; Thomas, C.; Da Costa, P.; Djéga-Mariadassou, G. On the Role of Organic Nitrogen-containing Species as Intermediates in the Hydrocarbon-assisted SCR of NO_x. *Appl. Catal. B* **2004**, *54*, 69-84.

(8) Tamm, S.; Fogel, S.; Gabrielsson, P.; Skoglundh, M.; Olsson, L. The Effect of the Gas Composition on Hydrogen-assisted NH_3-SCR over Ag/Al_2O_3. *Appl. Catal. B* **2013**, *136*, 168-176.

(9) Shimizu, K. I.; Shibata, J.; Yoshida, H.; Satsuma, A.; Hattori, T. Silver-alumina Catalysts for Selective Reduction of NO by Higher Hydrocarbons: Structure of Active Sites and Reaction Mechanism. *Appl. Catal. B* **2001**, *30*, 151-162.

(10) Noto, T.; Murayama, T.; Tosaka, S.; Fujiwara, Y. Mechanism of NO_x Reduction by Ethanol on a Silver-base Catalyst. *SAE Trans.* **2001**, 1187-1194.

(11) Yu, Y. B.; Gao, H. W.; He, H. FTIR, TPD and DFT Studies of Intermediates on Ag/Al_2O_3 During the Selective Catalytic Reduction of NO by C_2H_5OH. *Catal. Today*, **2004**, *93*, 805-809.

(12) Burch, R.; Breen, J. P.; Meunier, F. C. A Review of the Selective Reduction of NO_x with Hydrocarbons under Lean-burn Conditions with Non-zeolitic Oxide and Platinum Group Metal Catalysts. *Appl. Catal. B* **2002**, *39*, 283-303.

(13) Lee, J. H.; Schmieg, S. J.; Oh, S. H. Improved NO_x Reduction over the Staged Ag/Al_2O_3 Catalyst System. *Appl. Catal. A* **2008**, *342*, 78-86.

(14) Staroverov, V. N.; Scuseria, G. E.; Tao, J.; Perdew, J. P. Comparative Assessment of a New Nonempirical Density Functional: Molecules and Hydrogen-bonded Complexes. *J. Chem. Phys.* **2003**, *119*, 12129-12137.

(15) Andrae, D.; Haeussermann, U.; Dolg, M.; Stoll, H.; Preuss, H. Energy-adjusted Ab Initio Pseudopotentials for the Second and Third Row Transition Elements. *Theor. Chim. Acta* **1990**, *77*, 123-141.

(16) Xu, X.; Nakatsuji, H.; Lu, X.; Ehara, M.; Cai, Y.; Wang, N. Q.; Zhang, Q. E. Cluster Modeling of Metal Oxides: Case Study of MgO and the CO/MgO Adsorption System. *Theor. Chem. Acc.* **1999**, *102*, 170-179.

(17) Gu, J.; Wang, J.; Leszczynski, J. Structure and Energetics of (111) Surface of γ-Al_2O_3: Insights from DFT Including Periodic Boundary Approach. *ACS Omega* **2018**, *3*, 1881-1888.

(18) Digne, M.; Sautet, P.; Raybaud, P.; Euzen, P.; Toulhoat, H. Use of DFT to Achieve a Rational Understanding of Acid–basic Properties of γ-alumina Surfaces. *J. Catal.* **2004**, *226*, 54-68.

(19) Krishnan, R. B.; Binkley, J. S.; Seeger, R.; Pople, J. A. Self-consistent Molecular Orbital Methods. XX. A Basis Set for Correlated Wave Functions. *J. Chem. Phys.* **1980**, *72*, 650-654.

(20) McLean, A. D.; Chandler, G. S. Contracted Gaussian Basis Sets for Molecular Calculations. I. Second Row Atoms, Z= 11–18. *J. Chem. Phys.* **1980**, *72*, 5639-5648.

(21) Pople, J. A.; Head-Gordon, M.; Raghavachari, K. Quadratic Configuration Interaction. A General Technique for Determining Electron Correlation Energies. *J. Chem. Phys.* **1987**, *87*, 5968-5975.

(22) Wadt, W. R.; Hay, P. J. Ab Initio Effective Core Potentials for Molecular Calculations. Potentials for Main Group Elements Na to Bi. *J. Chem. Phys.* **1985**, *82*, 284-298.

(23) Giordano, L.; Pacchioni, G.; Bredow, T.; Sanz, J. F. Cu, Ag, and Au Atoms Adsorbed on TiO_2 (110): Cluster and Periodic Calculations. *Surf. Sci.* **2001**, *471*, 21-31.

(24) Mazheika, A. S.; Matulis, Vitaly E.; Ivashkevich, O. A. Quantum Chemical Study of Adsorption of Ag_2, Ag_4 and Ag_8 on Stoichiometric TiO_2 (110) Surface. *J. Mol. Struct.: THEOCHEM* **2010**, *942*, 47-54.

(25) Boys, S. F.; Bernardi, F. Calculation of Small Molecular Interactions by Differences of Separate Total Energies – Some Procedures with Reduced Errors. *Mol. Phys.* **1970**, *19*, 553-566.

(26) Frisch, M. J.; Trucks, G. W.; Schlegel, H. B.; Scuseria, G. E.; Robb, M. A.; Cheeseman, J. R.; Scalmani, G.; Barone, V.; Petersson, G. A.; Nakatsuji, H.; et al. *Gaussian 16*, Revision B.; Gaussian, Inc., Wallingford, CT, 2016.

(27) Peterson, K. A.; Puzzarini, C. Systematically Convergent Basis Sets for Transition Metals. II. Pseudopotential-based Correlation Consistent Basis Sets for the Group 11 (Cu, Ag, Au) and 12 (Zn, Cd, Hg) Elements. *Theor. Chem. Acc.* **2005**, *114*, 283-296.

(28) Beutel, V.; Krämer, H. G.; Bhale, G. L.; Kuhn, M.; Weyers, K.; Demtröder, W. High-resolution Isotope Selective Laser Spectroscopy of Ag_2 Molecules. *J. Chem. Phys.* **1993**, *98*, 2699-2708.

(29) Perdew, J. P.; Wang, Y. Accurate and Simple Analytic Representation of the Electron-gas Correlation Energy. *Phys. Rev. B* **1992**, *45*, 13244.

(30) Zhao, Y.; Truhlar, D. G. The M06 Suite of Density Functionals for Main Group Thermochemistry, Thermochemical Kinetics, Noncovalent Interactions, Excited States, and Transition Elements: Two New Functionals and Systematic Testing of Four M06-class Functionals and 12 Other Functionals. *Theor. Chem. Acc.* **2008**, *120*, 215-241.

(31) Adamo, C.; Barone, V. Toward Reliable Density Functional Methods without Adjustable Parameters: The PBE0 Model. *J. Chem. Phys.* **1999**, *110*, 6158-6170.

(32) Hay, P. J.; Wadt, W. R. Ab Initio Effective Core Potentials for Molecular Calculations. Potentials for the Transition Metal Atoms Sc to Hg. *J. Chem. Phys.* **1985**, *82*, 270-283.

(33) Roy, L. E.; Hay, P. J.; Martin, R. L. Revised Basis Sets for the LANL Effective Core Potentials. *J. Chem. Theory Comput.* **2008**, *4*, 1029-1031.

(34) Handschuh, H.; Cha, C. Y.; Bechthold, P. S.; Ganteför, G.; Eberhardt, W. Electronic Shells or Molecular Orbitals: Photoelectron Spectra of Ag_n^- Clusters. *J. Chem. Phys.* **1995**, *102*, 6406-6422.

(35) Duanmu, K.; Truhlar, D. G. Validation of Methods for Computational Catalyst Design: Geometries, Structures, and Energies of Neutral and Charged Silver Clusters. *J. Phys. Chem. C* **2015**, *119*, 9617-9626.

(36) Matulis, V. E.; Ivashkevich, O. A.; Gurin, V. S. DFT Study of Electronic Structure and Geometry of Neutral and Anionic Silver Clusters. *J. Mol. Struct.: THEOCHEM* **2003**, *664*, 291-308.

(37) Filatova, E. O.; Konashuk, A. S. Interpretation of the Changing the Band Gap of Al_2O_3 Depending on its Crystalline Form: Connection with Different Local Symmetries. *J. Phys. Chem. C* **2015**, *119*, 20755-20761.

(38) Nigam, S.; Majumder, C. Growth Pattern of Ag n (n= 1− 8) Clusters on the α-Al_2O_3 (0001) Surface: A First Principles Study. *Langmuir* **2010**, *26*, 18776-18787.

(39) Mazheika, A. S.; Matulis, V. E.; Ivashkevich O. A. Density Functional Study of Adsorption of Ag_n (n= 2, 4, 8) on Partially Reduced TiO_2 (1 1 0) Surface. *J. Mol. Struct.: THEOCHEM* **2010**, *950*, 46-52.

(40) Mazheika, A. S.; Bredow, T.; Matulis, V. E.; Ivashkevich, O. A. Theoretical Study of Adsorption of Ag Clusters on the Anatase TiO_2 (100) Surface. *J. Phys. Chem. C* **2011**, *115*, 17368-17377.

(41) Mazheika, A. S.; Bredow, T.; Ivashkevich, O. A.; Matulis, V. E. Theoretical Study of NO Conversion on Ag/TiO_2 Systems. II. Rutile (110) Surface. *J. Phys. Chem. C* **2012**, *116*, 25274-25285.

(42) Chen, B. W.; Kirvassilis, D.; Bai, Y.; Mavrikakis, M. Atomic and Molecular Adsorption on Ag (111). *J. Phys. Chem. C* **2018**, *123*, 7551-7566.

(43) He, H.; Yu, Y. Selective Catalytic Reduction of NO_x over Ag/Al_2O_3 Catalyst: from Reaction Mechanism to Diesel Engine Test. *Catal. Today* **2005**, *100*, 37-47.

(44) Glendening, E. D.; Halpern, A. M. Ab Initio Calculations of Nitrogen Oxide Reactions: Formation of N_2O_2, N_2O_3, N_2O_4, N_2O_5, and N_4O_2 from NO, NO_2, NO_3, and N_2O. *J. Chem. Phys.* **2007**, *127*, 164307.

(45) Rochana, P.; Lee, K.; Wilcox, J. Nitrogen Adsorption, Dissociation, and Subsurface Diffusion on the Vanadium (110) Surface: A DFT Study for the Nitrogen-selective Catalytic Membrane Application. *J. Phys. Chem. C* **2014**, *118*, 4238-4249.

(46) Tamijani, A. A; Salam, A.; de Lara-Castells, M. P. Adsorption of Noble-gas Atoms on the TiO_2 (110) surface: An Ab Initio-assisted Study with van der Waals-corrected DFT. *J. Phys. Chem. C* **2016**, *120*, 18126-18139.

TOC Graphics